

# Computer simulations of peritoneal fluid transport in CAPD

BENGT RIPPE, GUNNAR STELIN, and BÖRJE HARALDSSON

Department of Nephrology, University Hospital of Lund, Lund; Department of Nephrology, Sahlgrenska Hospital, Göteborg; and Department of Physiology, University of Göteborg, Göteborg, Sweden

**Computer simulations of peritoneal fluid transport in CAPD.** To model the changes in intraperitoneal dialysate volume (IPV) occurring over dwell time under various conditions in continuous ambulatory peritoneal dialysis (CAPD), we have, using a personal computer (PC), numerically integrated the phenomenological equations that describe the net ultrafiltration (UF) flow existing across the peritoneal membrane in every moment of a dwell. Computer modelling was performed according to a three-pore model of membrane selectivity as based on current concepts in capillary physiology. This model comprises small “paracellular” pores (radius  $\approx 47 \text{ \AA}$ ) and “large” pores (radius  $\approx 250 \text{ \AA}$ ), together accounting for  $\approx 98\%$  of the total UF-coefficient ( $L_pS$ ), and also “transcellular” pores (pore radius  $\approx 4$  to  $5 \text{ \AA}$ ) accounting for  $1.5\%$  of  $L_pS$ . Simulated curves made a good fit to IPV versus time data obtained experimentally in adult patients, using either  $1.36$  or  $3.86\%$  glucose dialysis solutions, under control conditions; when the peritoneal UF-coefficient was set to  $0.082 \text{ ml/min/mm Hg}$ , the glucose reflection coefficient was  $0.043$  and the peritoneal lymph flow was set to  $0.3 \text{ ml/min}$ . Also, theoretical predictions regarding the IPV versus time curves agreed well with the computer simulated results for perturbed values of effective peritoneal surface area,  $L_pS$ , glucose permeability-surface area product (PS or “MTAC”), intraperitoneal dialysate volume and dialysate glucose concentration. Thus, increasing the peritoneal surface area caused the IPV versus time curves to peak earlier than during control, while the maximal volume ultrafiltered was not markedly affected. However, increasing the glucose PS caused both a reduction in the IPV versus time curve “peak time” and in the “peak height” of the curves. The latter pattern was also seen when the dialysate volume was reduced. It is suggested that computer modelling based on a three-pore model of membrane selectivity may be a useful tool for describing the IPV versus time relationships under various conditions in CAPD.

The exchange characteristics of the peritoneal membrane vary greatly among individual patients on continuous ambulatory peritoneal dialysis (CAPD) [1, 2]. After years of PD treatment many patients develop an increased peritoneal glucose clearance, which will reduce their capacity of removing fluid by ultrafiltration (osmosis), on ordinary dialysis prescriptions [3–7]. To manage these patients it is essential to have knowledge of the factors that determine the exchange of fluid across the peritoneal membrane, and hence, the variation in intraperitoneal dialysate volume (IPV) over cycle time.

In a previous study we have discussed the principal phenomenological membrane coefficients necessary to describe the IPV versus time relationships under ordinary conditions [8]. The

major factors affecting the IPV versus time curves are: the peritoneal osmotic conductance to glucose, that is, the product of the peritoneal UF-coefficient ( $L_pS$ ) and the glucose osmotic reflection coefficient ( $\sigma_g$ ), the glucose permeability surface area product ( $PS_g$ ), the peritoneal lymph flow ( $L$ ), and finally, the intraperitoneal glucose concentration and dialysate volume at the start of each cycle, respectively [8–11].

From the phenomenological equations described previously [8] it is possible to predict in approximate terms how the IPV versus time curve during a single dwell will vary in response to variation in the factors mentioned above. In the present paper we deal with the issue more pragmatically, using a personal computer (PC) to simulate IPV versus time curves under standard conditions and for perturbed values of effective peritoneal surface area, peritoneal UF-coefficient, glucose mass-transfer area coefficient (MTAC or PS), dialysate volume, etc. Model parameters for these computer simulations are based on a “three-pore” model of membrane selectivity presented previously and derived from capillary physiology [12–15]. This model has proven to be a useful tool for describing transvascular and transperitoneal exchange of small and large solutes. According to the model the peritoneum behaves as a membrane having a large number of “small pores” (radius  $40$  to  $60 \text{ \AA}$ ), accounting for  $90$  to  $95\%$  of the total hydraulic conductance (UF-coefficient), and a very low number (1 part per  $15,000$  small pores) of “large pores” (radius  $200$  to  $300 \text{ \AA}$ ), accounting for approximately  $5\%$  of the peritoneal UF-coefficient [12, 13]. In addition, a third transperitoneal exchange route is predicted to exist, namely a transcellular (“ultra-small” pore) pathway, accounting for  $1$  to  $2\%$  of the total UF-coefficient and having an approximate pore radius of  $4$  to  $5 \text{ \AA}$  [12, 14–16].

## Methods

### Theory

During a peritoneal dialysis dwell the instantaneous net volume flow occurring through the peritoneal membrane

$$\left( J_v \text{ or } \frac{dV}{dt} \right)$$

<sup>1</sup>  $\sigma$  is defined as the fractional “effective” osmotic pressure exerted by a solute across the membrane investigated in relation to its “ideal” osmotic pressure as established for a perfectly semipermeable membrane.

can be described according to the following phenomenological equation [17]:

$$\frac{dV}{dt} = J_v = L_p S (\Delta P - \sigma_{\text{prot}} \Delta \pi_{\text{prot}} - \sigma_g \Delta \pi_g - \sum_{i=1}^n \sigma_i \Delta \pi_i) - L \quad (1)$$

where  $L_p S$  has been defined above and where  $\Delta P$  represents the mean hydrostatic pressure difference between the blood capillaries and the peritoneal cavity.  $\Delta \pi_{\text{prot}}$  is the transperitoneal colloid osmotic pressure difference caused by the plasma proteins, and  $\sigma_{\text{prot}}$  and  $\sigma_g$  represent the average osmotic reflection coefficients for total protein and glucose across the peritoneum, respectively.  $\Delta \pi_g$  is the ideal peritoneal crystalloid osmotic pressure difference exerted by glucose across a semipermeable membrane. The fourth term in the parenthesis denotes the sum of all other "effective" crystalloid osmotic gradients acting across the peritoneal membrane. Finally,  $L$  represents the lymph flow from the peritoneal cavity to the blood, whereas  $V$  stands for volume and  $t$  for time.

The crystalloid osmotic pressure differences acting across the peritoneal membrane initially after infusion of a (glucose) dialysis solution into the peritoneal cavity,  $\Delta \pi_g$  and,

$$\sum_{i=1}^n \Delta \pi_i$$

will dissipate exponentially with time due to solute diffusion across the membrane [8–11, 18]. Hence, equation 1 contains several exponential crystalloid osmotic pressure terms, having the "lumped" rate constant "k" ( $\text{min}^{-1}$ ). The other terms, ( $\Delta P$ ,  $\sigma_{\text{prot}} \Delta \pi_{\text{prot}}$ , and  $L$ ) will, however, remain more or less constant over time during a dwell.

Assuming that equation 1 contains one "lumped" exponential term, describing the dissipation of the effective osmotic gradients acting across the peritoneum, and a number of constants, it can be integrated analytically [18] yielding:

$$V_t = V_o + a_1(1 - e^{-kt}) - a_2 t \quad (2)$$

where  $V_t$  represents the drained dialysate volume, expressed as a function of time.  $V_o$  is the volume instilled at time zero, and  $a_1$ ,  $a_2$  and  $k$  are some arbitrary coefficients that determine the change occurring in  $V_t$  as a function of time.

Stelin and Rippe [8] showed that if glucose acts as the major crystalloid osmotic agent during CAPD, which is a reasonable assumption, then

$$a_1 \propto \frac{L_p S \sigma_g}{PS_g} \Delta C_{g_o} \bar{V} \quad (3)$$

where  $PS_g$  is the glucose mass transfer area coefficient (MTAC),  $\Delta C_{g_o}$  is the transperitoneal glucose concentration gradient existing at time zero and  $\bar{V}$  represents the mean i.p. volume during the dwell. The coefficient  $a_1$  represents the maximal fluid volume that can be transported into the peritoneal cavity by glucose-induced osmosis during a dwell, when both lymphatic

**Table 1.** Parameters used for computer simulations of  $V(t)$  versus time curves according to a three-pore model of membrane selectivity

Small pore radius ( $r_s$ )	47 Å
Large pore radius ( $r_L$ )	250 Å
Fractional small pore UF-coeff ( $\alpha_s$ )	0.935
Fractional transcellular UF-coeff ( $\alpha_c$ )	0.015
Fractional large pore UF-coeff ( $\alpha_L$ )	0.050
Fractional large pore surface area	0.002
Mol radius of sodium (and chloride)	2.3 Å
Mol radius of urea	2.6 Å
Mol radius of glucose	3.7 Å
Mol radius of albumin ("total protein")	35.5 Å
UF-coefficient ( $L_p S$ )	0.082 ml/min/mm Hg
Osmotic conductance to glucose ( $L_p S \sigma_g$ )	3.5 $\mu\text{l}/\text{min}/\text{mm Hg}$
Unrestricted pore area over unit diffusion distance ( $A_o/\Delta x$ )	27,000 $\text{cm}^2$
PS (MTAC) for glucose	15.5 ml/min
Peritoneal lymph flow (L)	0.3 ml/min
Transperitoneal hydrostatic pressure gradient ( $\Delta P$ )	9 mm Hg
Transperitoneal oncotic pressure gradient ( $\Delta \pi_{\text{prot}}$ )	22 mm Hg
Dialysis fluid volume instilled	2,050 ml
Peritoneal residual volume	300 ml
Serum urea conc	20 mmol/liter
Serum sodium (and corresponding anion) conc	140 mmol/liter
Dialysis fluid sodium conc	132 mmol/liter
Serum glucose conc	6.5 mmol/liter

Reflection coefficients for all solutes in the transcellular pathway were set to 1. A majority of simulations were performed for 3.86% glucose in the dialysis fluid infused.

and capillary fluid absorption to the blood are set to zero. Thus  $a_1$  describes the "height" of the  $V_t$  (or IPV) versus time curve. Furthermore, "k" approximately equals  $PS_g/\bar{V}$ . It was also shown previously [8] that the time at which the  $V_t$  curve peaks ( $t_{\text{peak}}$ ) is inversely proportional to "k", or in terms of PS and  $\bar{V}$ :

$$t_{\text{peak}} \propto \frac{\bar{V}}{PS_g} \quad (4)$$

Note also that the absorption of fluid from the peritoneal cavity to the blood ( $a_2$ ) is dependent on the sum of the peritoneal lymph flow (L) and the capillary fluid absorption due to  $L_p S$  and the capillary "Starling forces", that is, the "effective" transperitoneal colloid osmotic pressure difference and the transperitoneal hydrostatic pressure difference [8, 12, 19, 20]:

$$a_2 = L_p S (\sigma_{\text{prot}} \Delta \pi_{\text{prot}} - \Delta P) + L \quad (5)$$

#### Computation techniques

In this paper we have tested the validity of equations 2 to 5 by numerically integrating equation 1 using a personal computer (Casio FX-860 P). A step-wise iterative procedure was employed for the integration, using the parameters listed in Table 1. Parameter values including those for  $\Delta \pi_{\text{prot}}$ ,  $\Delta P$ ,  $L$  and  $L_p S$  were taken from our previous studies [8, 12]. Crystalloid osmotic gradients for glucose, urea, sodium and "sodium anions" (lactate, chloride) were taken into account, but those for potassium, magnesium, phosphate, etc., were neglected.

The iterative procedure followed included: 1) computation of the i.p. concentrations of glucose, urea and sodium (+chloride) at the start of a short time interval ( $\Delta t$ ) of iteration (1 min); 2) assessment of the transperitoneal volume flow ( $J_v$ ) during that period; 3) computation of the increment in peritoneal volume ( $\Delta V$ ) during  $\Delta t$ ; 4) calculation of the new IPV [ $V(t + \Delta t)$ ]; and 5) starting a new iteration. Each iteration step can be described by:

$$V(t + \Delta t) = V(t) + L_p S \Delta t [\Delta P(V) - \sigma_{\text{prot}} \Delta \pi_{\text{prot}} - \sigma_g \Delta \pi_g(t) - \sigma_u \Delta \pi_u(t) - \sigma_{\text{Na}} \Delta \pi_{\text{Na}}(t) - \sigma_{\text{an}} \Delta \pi_{\text{an}}(t)] - L \Delta t \quad (6)$$

where u, Na and an stand for urea, sodium and its anions (chloride and lactate), respectively. With negligible error, the sum of the last two crystalloid osmotic transients within parenthesis can be numerically treated as twice the sodium osmotic transient. This approach was taken in this study. The crystalloid osmotic gradients included in equation 6, that is,  $\Delta \pi_g$ ,  $\Delta \pi_u$ ,  $\Delta \pi_{\text{Na}}$  and  $\Delta \pi_{\text{an}}$ , all change with time during the course of the dialysis (see eq. 9) as indicated in the equation. The change in  $\Delta P$  (in mm Hg) with intraperitoneal volume ( $V$ ) in this study [denoted  $\Delta P(V)$ ] was simulated according to the relationship between intraperitoneal pressure and dialysate volume obtained by Twardowski et al for the sitting position [21]:

$$\Delta P(V) = \Delta P(V_0) - \frac{V_t - V_0}{490} \quad (7)$$

where  $\Delta P(V_0)$  was set to 9 mm Hg and  $V_0$  to 2,050 ml. Furthermore, according to van't Hoff's law the ideal crystalloid osmotic gradients acting across the peritoneal membrane are related to the transperitoneal concentration gradients by:

$$\Delta \pi = RT [C_p - C_D(t)] \quad (8)$$

where  $RT$  is the product of the gas constant and the temperature in degrees Kelvin (19.3 mm Hg/mmol/liter) and where  $C_p$  is the plasma solute concentration and  $C_D$  the concentration of solute in the dialysate as a function of time.

Initial ( $t = 0$ ) i.p. solute concentration [ $C_D(0)$ ] was calculated from the solute concentration in the dialysis fluid prior to instillation ( $C_{\text{DS}}$ ), the plasma solute concentration ( $C_p$ ) and also from the residual i.p. volume ( $V_R$ ) and the dialysis fluid volume ( $V_0$ ):

$$\frac{V_0 \cdot C_{\text{DS}} + V_R \cdot C_p}{V_0 + V_R} = C_D(0) \quad (9)$$

The alterations in  $C_D$  with time [ $C_D(t)$ ] was obtained from simple mass balance considerations. During a short time interval ( $\Delta t$ ) the change in  $C_D$  for either glucose, urea or sodium chloride [from  $C_D(t)$  to  $C_D(t + \Delta t)$ ] is obtained from:

$$V(t + \Delta t) \cdot C_D(t + \Delta t) = C_D(t) \cdot V(t) + Cl(C_p - C_D(t)) \Delta t \quad (10)$$

where  $V(t)$  here includes the residual volume ( $V_R$ ) and where  $Cl$  is the "unidirectional" peritoneal clearance of solute (12) as defined by:

$$Cl = \frac{J_v (1 - \sigma_s)}{1 - e^{-Pe}} \quad (11)$$

In this non-linear [22] flux equation, as modified to describe unidirectional transport,  $Pe$  is a modified Peclet number, that is,  $Pe = J_v (1 - \sigma_s) / PS$  and  $\sigma_s$  is the osmotic small pore reflection coefficient of the solute (eq. 13). During control, small solute  $PS$  values, with the exception of  $PS$  for glucose, were calculated for an "unrestricted" pore area over unit diffusion distance ( $A_0/\Delta x$ ) of 27,000 cm consistent with current results from peritoneal equilibration tests (PET) [1, 23].  $PS$  for glucose had to be increased from 10.2 ml/min (as predicted for  $A_0/\Delta x = 27,000$ ) to 15.5 ml/min to make experimental data fit the model.  $J_v$  is the transperitoneal volume flow occurring through small pores [12] as obtained by:

$$J_{v_s} = \alpha_s L_p S [\Delta P(V) - \sigma_{\text{prot},s} \Delta \pi_{\text{prot}} - \sigma_{g,s} \Delta \pi_g(t) - \sigma_{u,s} \Delta \pi_u(t) - 2 \cdot \sigma_{\text{Na},s} \Delta \pi_s(t)] \quad (12)$$

where  $s$  stands for small pores, and where  $\alpha_s$  is the fraction of total hydraulic conductance accounted for by small pores. In a similar way, the large pore and the transcellular volume flows,  $J_{v_L}$  and  $J_{v_c}$ , can be obtained [12] by inserting the appropriate values of  $\alpha$  (fractional hydraulic conductance) and  $\sigma$  for every solute and pore size (compare with Table 1).

Osmotic reflection coefficients were calculated from the expression [24]:

$$\sigma = 16/3 \gamma^2 - 20/3 \gamma^3 + 7/3 \gamma^4 \quad (13)$$

where  $\gamma$  is solute radius over pore radius for either small or large pores.  $\sigma$  for the transcellular (ultra-small pore) pathway was set to unity for all solutes considered. For the three-pore model employed here the average reflection coefficients for the entire heteroporous membrane (in eq. 1) due to small pore ( $s$ ), large pore ( $L$ ) and transcellular ( $c$ ) partial  $\sigma$ 's, respectively, are weighted by the respective fractional hydraulic conductances accounted for by either pore system, that is, by  $\alpha_s$ ,  $\alpha_L$  and  $\alpha_c$ . Thus (since  $\sigma_c = 1$ ):

$$\sigma = \alpha_c + \alpha_s \sigma_s + \alpha_L \sigma_L \quad (14)$$

This treatment of transperitoneal fluid transport using lumped reflection coefficients is equivalent to using equation 1 (omitting  $L$ ) separately for either of the peritoneal fluid conductive pathways (compare with eq. 12) and then summing up the *partial* volume flows ( $J_{v_s}$ ,  $J_{v_L}$ ,  $J_{v_c}$ ) and the lymph flow ( $L$ ) to obtain the net fluid flow ( $J_v$ ) across the peritoneal membrane.

The dialysate osmolality was calculated as the sum of the computed i.p. glucose, urea and twice the sodium concentrations in the dialysate. It was then assumed that sodium chloride and sodium lactate are fully dissociated compounds, which is not quite correct. On the other hand, we did not take into account the presence of i.p. calcium, magnesium, etc., so the total dialysate osmolality will hardly be overestimated.

## Results

### Control conditions

*Effects of variations of the glucose concentration in the dialysis solution.* Figure 1 shows computer simulated drained volume versus time [ $V(t)$ ] curves obtained by varying the glucose concentration in the dialysis solution and using the parameters listed in Table 1. Setting  $PS$  for glucose at 15.5

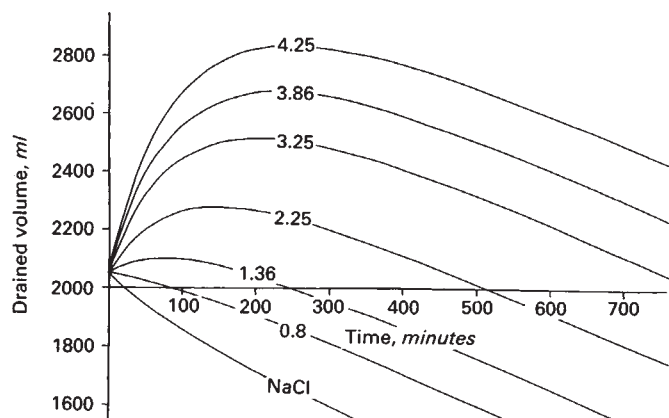


**Fig. 1.** Computer simulated drained volume versus time  $[V(t)]$  curves for varying glucose concentrations in the dialysate. Parameters used for the simulations are listed in Tables 1 and 2. Glucose concentrations in the dialysis solution infused are varied from zero (NaCl curve) to 4.25%.

ml/min makes the curves fit nearly exactly to our previously published experimental drained volume versus time relationships for 3.86 and 1.36% glucose in the dialysis solution [8]. The value of glucose PS of 15.5 ml/min was employed for control conditions throughout this study. This rather "high"  $PS_g$  as selected to fit the model to our previous data is discussed below.

In the figure, the glucose concentration in the dialysis solution (prior to instillation) is altered from zero (NaCl curve) to 4.5%. The  $V(t)$  curves largely follow the predictions of equation 3. Thus it is mainly the "height" of the curves ( $a_1$ ) that increases with increasing glucose concentration and  $\Delta C_{g_0}$ . To a lesser extent, however, the time at which the  $V(t)$  curves peak ( $t_{peak}$ ) also increases with increasing dialysate glucose concentration.

*Dialysate sodium, glucose and total osmolality versus time during cycles with either 1.36 or 3.86% glucose in the dialysis fluid.* Due to the heteroporous nature of the peritoneal membrane such as predicted by the present three-pore model, a considerable fraction (40 to 50%) of the transperitoneal osmotic fluid flow induced by a large glucose osmotic gradient will occur through the "ultra-small pore" (transcellular) peritoneal pathway. Thus, even though the peritoneal membrane is highly permeable to small solutes, there will be a sieving of small solutes (mainly sodium chloride) across the peritoneum during the first few hours of the dwell. This is illustrated in Figure 2. This figure depicts the computer simulated sodium concentration in the dialysate as a function of time for 1.36 or 3.86% glucose in the dialysis fluid. Plasma sodium concentration is set at 140 mmol/liter.

Note that the sodium concentration in the dialysate reaches a minimum (of 118.5 mmol/liter) at 90 minutes for the 3.86% (glucose) dialysis fluid and of 132 mmol/liter at approximately 50 minutes for the 1.36% solution, respectively. Furthermore, for the 3.86% solution the dialysate sodium concentration lies below that in plasma during more than nine hours of the dwell! This general pattern is very close to that recently reported by Heimbürger et al [7] during 3.86% Dianeal® dwells in CAPD patients. The "normal" patients in that study reached a mini-

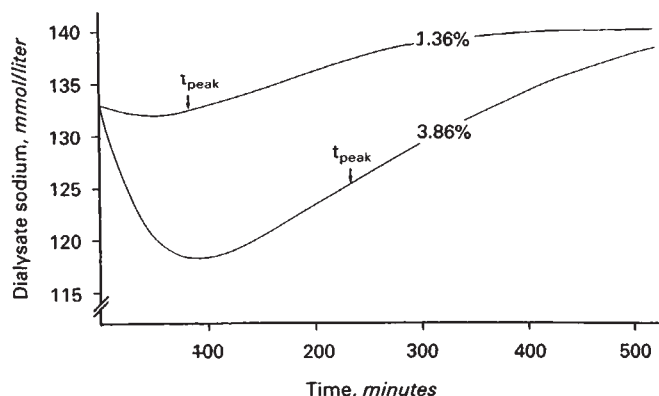


**Fig. 2.** Computer simulated sodium concentration in the dialysate as a function of dwell time for 1.36 per cent (upper curve) and 3.86% (lower curve) glucose dialysis solutions during control conditions. Initial dialysate sodium concentration (after mixing of the dialysis fluid with the residual volume) is 133 mmol/liter and that in plasma is 140 mmol/liter (Table 1). Peak times ( $t_{peak}$ ) of the corresponding  $V(t)$  curves (Fig. 1) are also indicated in the figure.

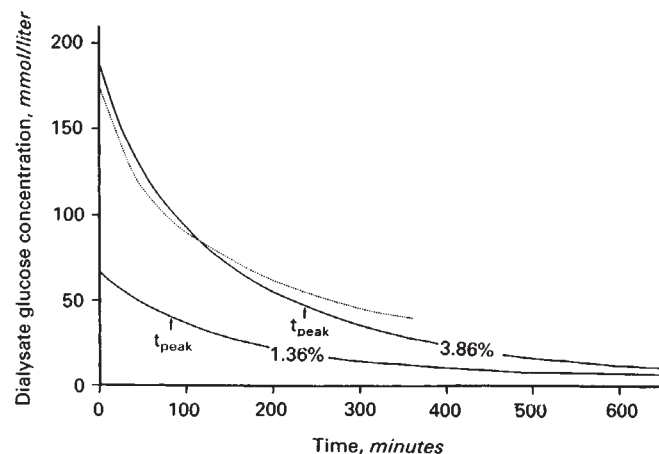


**Fig. 3.** Simulated dialysate glucose concentrations versus dwell time during 3.86% and 1.36% (glucose) dwells under control conditions. The 1.36% curve is identical to that recently published for the "distributed transport model" by Seames et al [26]. The 3.86% curve deviates from that measured in CAPD patients having "normal" UF-characteristics by Heimbürger et al [7] (dotted line). Peak times of the corresponding  $V(t)$  curves ( $t_{peak}$ ) are indicated in the figure.

mum dialysate sodium concentration after 90 min of the dwell of approximately  $120.5 \pm 3.5$  ( $\pm$ SD) mmol/liter.

The computer simulated reductions in dialysate glucose concentration versus time for 1.36% and 3.86% glucose dialysis fluid dwells, respectively, are shown in Figure 3. For the 3.86% solution measured values for normal CAPD patients from the study of Heimbürger et al [7] are indicated by a dotted line. The simulated curve for the 1.36% solution is (nearly) identical to that calculated using a "distributed model" [25] of fluid and mass transfer, such as that recently published by Seames, Moncrief and Popovich [26]. From the mentioned study and the present one it seems evident that both the present (parallel pathway) model and distributed models *underestimate* the i.p. glucose concentration after approximately 120 minutes of the

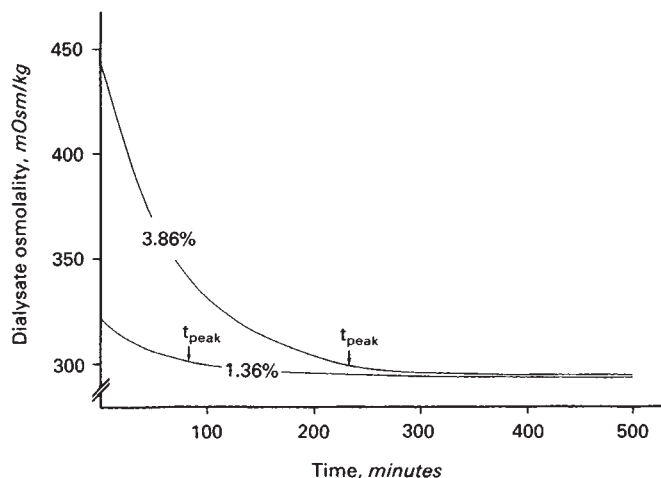


Fig. 4. Simulated dialysate osmolality over dwell time during control conditions for 3.86% (upper curve) and 1.36% (lower curve) glucose dialysis solutions, respectively. Curve peak times ( $t_{\text{peak}}$ ) are indicated in the figure.

dwell. Note also that the  $t_{\text{peak}}$  occurs long before the i.p. glucose concentration reaches plasma values.

As presented in Figures 2 and 3, the i.p. glucose and sodium chloride concentrations both fall during the first 60 to 90 minutes of the dwell. Later during the cycle, the concentration of sodium and its anions (chloride and lactate) will increase while there is a continuing fall in i.p. glucose concentration. Hence, the initial rapid fall in dialysate osmolality, partly occurring due to dilution, partly due to glucose diffusion, slows down considerably after 50 to 90 minutes. This is illustrated in Figure 4, showing the simulated dialysate osmolality versus time for 1.36% and 3.86% (glucose) dialysates. The general pattern shown here agrees well with that measured in normal CAPD patients [7, 11].

#### Effects on i.p. volume versus time $[V(t)]$ curves of variations of peritoneal surface area (S)

The effective peritoneal exchange surface area may increase in CAPD patients due to, for example, capillary "recruitment," implying that the number of effectively perfused capillaries is increased. This is usually seen in inflammation (compare with peritonitis). Decreases in S may occur due to, for instance, formations of peritoneal adhesions.

Figure 5 demonstrates the effect of altering the peritoneal surface area on  $V(t)$  curves simulated for 3.86% glucose in the dialysis fluid, from control, as denoted in the curve by "1.0," up to 10 times control and down to 0.1 times control. Note, that despite large variations in S, the height of the curves ( $a_1$ ), as predicted from equation 3, is relatively well maintained. This is probably because S is part of both the numerator and denominator of the expression to the right in equation 3. However, since the  $t_{\text{peak}}$  is inversely related to  $PS_g$  (equation 4), it will decrease with increasing peritoneal surface area. Thus the theoretical predictions made from equation 3 and 4 are in good agreement with the results of the computer assisted numerical integration of equation 1 when S is varied within a wide range.

#### Effects of variations in peritoneal UF-coefficient ( $L_pS$ )

According to equation 4, changes in  $L_pS$  will not significantly affect the  $t_{\text{peak}}$ . However, according to equation 3 the height of the  $V(t)$  curves should be highly dependent on  $L_pS$ . This is illustrated in Figure 6, showing the computer simulated results of varying  $L_pS$  on  $V(t)$  curves for 3.86% glucose in the dialysis fluid.  $L_pS$  is varied from 0.082 ml/min/mm Hg (control or "1.0") in the range of 0.1 to 1.7 times control. Note how small variations in  $L_pS$  markedly affect the height of the curves. Increases in  $L_pS$  implies increases both in the initial UF-rate and in the peritoneal-to-blood absorption rate ( $a_2$ ) ensuing upon the curve peak (compare with eq. 5).

#### Effects of variations in PS ("MTAC") for glucose $PS_g$

Increasing PS for glucose, while keeping  $L_pS$  at 0.082 ml/min/mm Hg, will, according to equations 3 and 4, reduce both the  $t_{\text{peak}}$  and the curve height ( $a_1$ ). This is illustrated in Figure 7 showing the computer simulated results for 3.86% glucose when PS for glucose is perturbed from control (15.5 ml/min denoted "1.0") to range from 0.5 to 3 times control. Note that an increased  $PS_g$  will markedly reduce the volume ultrafiltered during a 240 to 300 minutes (4 hr to 5 hr) dwell. The pattern of  $V(t)$  alterations seen when  $PS_g$  is increased relative to  $L_pS$  apparently mimics that shown by a certain number of patients who have been on CAPD for several years (3 to 7). Thus, quite few patients will present a reduced UF-capacity on long-term CAPD treatment.

#### Effects of variations in dialysis fluid volume ( $V_o$ ) and in peritoneal residual volume ( $V_R$ )

The computer simulated results of varying the fluid volume instilled for 3.86% glucose in the dialysis fluid when peritoneal residual volume is set to 300 ml, are shown in Figure 8. Again there is good agreement between simulations and theoretical predictions according to equations 3 and 4. Thus, an increased  $\bar{V}$  will increase both  $a_1$  and  $t_{\text{peak}}$ . Control curve is obtained for an instilled volume of 2,050 ml (2.05 liter), and curves simulated for infused volumes ranging from 1,050 ml (1.05 liter) up to 3,050 ml (3.05 liter) are shown for comparison.

Altering the residual volume will affect the transperitoneal glucose concentration at time zero ( $\Delta C_{g_0}$ ) as well as the total intraperitoneal volume. Thus, changing the residual volume would, according to equations 3 and 4, affect both the height of the curves and the  $t_{\text{peak}}$ . This is shown in Figure 9, where the i.p. residual volume is varied from 0 to 1,500 ml for an instilled volume is 2,050 ml and a glucose concentration in the dialysis fluid of 3.86%.

#### Effects of variations of peritoneal lymph flow (L)

An increased lymph flow partly offsets the dialysate's potential of removing body fluid by ultrafiltration (osmosis) during PD. In Figure 10 the computer simulated results of increasing L from 0 ml/min via "control", that is, 0.3 ml/min [8, 19, 27], to 2 ml/min [28, 29] during a 3.86% Dianeal® dwell is depicted. With this increase in L the total rate of fluid absorption from the peritoneal cavity to the blood increases from 0.90 to 2.9 ml/min, making the curve tails become steeper with increasing lymph flows. This pattern of  $V(t)$  alterations towards a reduced capacity of UF is different from that seen when PS for glucose alone

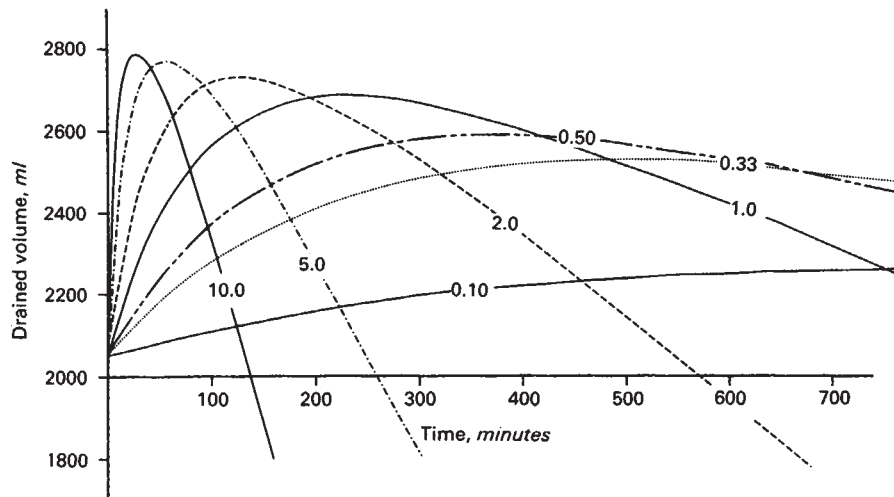


Fig. 5. Simulated  $V(t)$  curves as a function of surface area ( $S$ ) (eq. 3). Curves are simulated for 3.86% glucose in the dialysate. Control curve is denoted "1.0". Surface area is varied from 0.1 times control (denoted "0.10") to 10 times control (denoted "10.0").

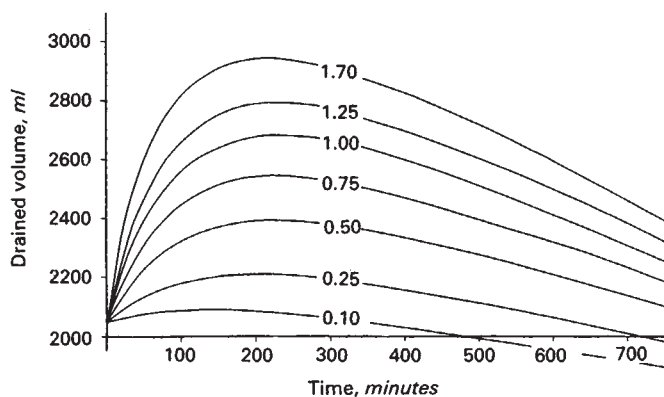


Fig. 6. Effect of varying  $L_pS$  from 0.1 times control (denoted 0.10) to 1.7 times control (denoted 1.70) on simulated  $V(t)$  versus time curves for 3.86% glucose in the dialysate infused.

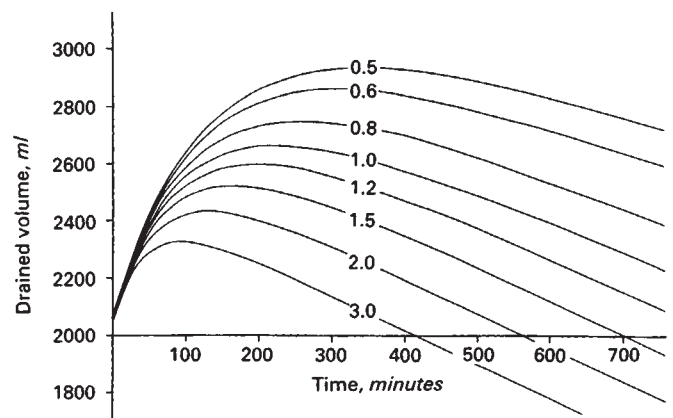


Fig. 7. Effects of varying  $PS_g$  for glucose ( $PS_g$ ) from 0.5 times control to 3 times control. Control curve (denoted 1.0) is generated for 3.86% glucose in the dialysate.

is increased. However, as shown previously [8], when the total peritoneal to blood absorption rate remains unaltered at control ( $\approx 1.2$  ml/min), then only a limited range of  $L$  values is theoretically possible (0.3 to 0.7 ml/min) under the provision that the peritoneal membrane "sieving coefficients" for small solutes are  $\geq 0.3$  [8].

#### Theoretical result of varying the small pore radius ( $r_s$ )

Inflammatory increases in microvascular permeability are usually the result of the formation of interendothelial gaps (large pores), preferentially in venular endothelium, caused by inflammatory mediators, such as histamine-type mediators and/or cytokines [30, 31]. It can be shown that large pore formation would not markedly affect the IPV versus time curves. Furthermore, the small pore system is usually not significantly affected by inflammation [30, 32]. Still it would be of theoretical interest to study how variations in  $r_s$  would affect the  $V(t)$  curves.

In Figure 11 the small pore radius is increased from  $36 \text{ \AA}$ , via  $47 \text{ \AA}$  (control curve) to  $80 \text{ \AA}$ , keeping the total pore area over unit diffusion distance ( $A_o/\Delta x$ ) constant at 27,000 cm. Again the simulations are made for 3.86% glucose in the dialysate. Note

that the  $t_{\text{peak}}$  will be reduced when  $r_s$  is increased, whereas there is a tendency that the height of the curves ( $a_1$ ) increase. This follows from equations 3 and 4. Increasing  $r_s$  will increase  $L_pS$  more than  $PS_g$ , since  $L_pS$  is related to the fourth power of  $r_s$  according to Poiseuille's law, while  $PS_g$  is related to  $r_s$  (via  $S$ ) by its second power. Furthermore,  $\sigma_g$  is related to  $r_s$  by equation 12. Thus, when  $r_s$  is increased, the numerator of the expression to the right in equation 3 will in most instances increase more than the denominator, provided that the fall in  $\sigma_g$  is small, and hence,  $a_1$  is increased. Furthermore, when  $r_s$  increases, then  $PS$  will increase, and hence, the  $t_{\text{peak}}$  is reduced.

#### Effects of simultaneously increasing peritoneal surface area ( $S$ ), the number of large pores ( $n_L$ ) and the peritoneal lymph flow ( $L$ )

During peritonitis the  $V(t)$  curves usually peak early (the  $t_{\text{peak}}$  is reduced). The height of the  $V(t)$  curves may decrease, increase or remain unchanged [4, 33, 34]. These changes may be simulated by simply increasing the number of effectively perfused capillaries, implying increases in the peritoneal surface

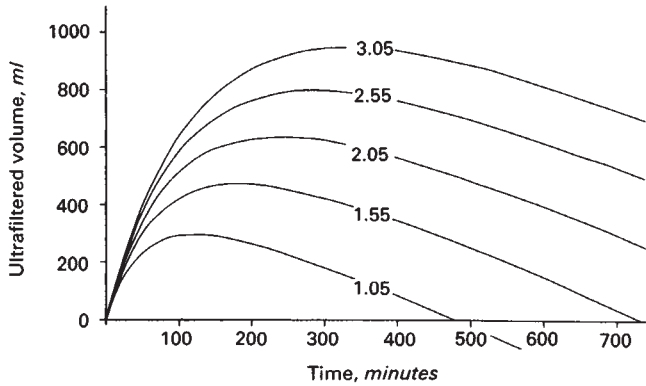


Fig. 8. Simulated ultrafiltered volume versus dwell time as a function of instilled dialysate volume, as varied from 1,050 ml to 3,050 ml. Control curve is generated for an instilled volume of 2,050 ml and a dialysate glucose concentration of 3.86%. Residual volume is 300 ml.

area (S). The effect of increasing S alone has been demonstrated in Figure 5. In peritonitis vascular permeability is also increased and, as mentioned above, this is usually due to an increase in large pore number, which will greatly enhance the leakage of proteins from the blood to the peritoneal cavity [30–33]. Furthermore, lymph flow (L) is expected to increase.

In Figure 12 simulations of V(t) curves are made for both 1.36% and 3.86% glucose in the dialysate. S is here increased by 70%. The ratio of large pore to small pore number is increased one order of magnitude (from 1/14,970 to 1/1,497). L is either unchanged at 0.3 ml/min (hatched line) or is increased to 1 ml/min (dotted line). Control curves for 1.36 and 3.86% glucose are represented by solid lines. As a result of these perturbations (regardless of the assumptions for L),  $L_pS$  was found to increase from 0.082 to 0.201 ml/min/mm Hg and  $\alpha_L$  increased from 0.05 to 0.35. Furthermore,  $\alpha_s$  dropped from 0.935 to 0.64 and  $\alpha_c$  decreased from 0.015 to 0.010. According to equation 14,  $\sigma$  for glucose ( $\sigma_g$ ) decreased from 0.043 to 0.030 and  $\sigma$  for Na dropped from 0.026 to 0.018. Simultaneously,  $\sigma$  for albumin fell from 0.90 to 0.64. Somewhat surprisingly, the shape of the IPV versus time curves was only little affected by the increase in large pore number.

Increasing the surface area (S) further than in this example will make the V(t) curves peak even earlier, and the steepness of the curve tails will increase further. If PS for glucose increases out of proportion to  $L_pS$ , then the curve height ( $a_1$ ) will tend to decrease. The specific example of changes in peritoneal exchange parameters compatible with peritonitis depicted here is, of course, just one of many possibilities. Increases in S, conceivably through recruitment of capillaries, seem, however, to play a key role in peritonitis, leading to a “leftward” displacement of the V(t) curves and an increased rate of fluid absorption ( $a_2$ ) from peritoneum to blood.

### Discussion

The present computer simulations of the variations in drained peritoneal dialysate volume as a function of time, V(t), during a single PD cycle are based on a three-pore model of peritoneal permselectivity. This model is founded on current concepts valid for transmucosal transport. The main elements of this heteroporous model are: the small pore (paracellular path-

way) radius ( $r_p$ ), the peritoneal UF-coefficient ( $L_pS$ ), the fractional UF-coefficient accounted for by small pores ( $\alpha_s$ ) and by a transcellular fluid conductive pathway ( $\alpha_c$ ), respectively, and the glucose permeability-surface area product ( $PS_g$  or  $MTAC_g$ ). To be able to model the absorption of fluid from the peritoneal cavity to the blood occurring after three to six hours, assumptions had also to be made concerning the peritoneal lymph flow (L) and the capillary “Starling forces” ( $\Delta P$  and  $\sigma_{prot} \Delta \pi_{prot}$ ). The major non-membrane parameters determining transperitoneal fluid exchange are: the volume and glucose concentration of the dialysate instilled (mass of glucose administered) and the residual intraperitoneal volume. Changes in large pore number of radius, at least within the range expected during inflammation, were not, however, found to markedly affect the peritoneal fluid balance. Neither did fluctuations of plasma solute concentrations (urea, glucose or sodium) within  $\pm 5$  mmoles/liter have any major influence on transperitoneal fluid exchange.

The computer assisted numerical integration of the functions describing the instantaneous transperitoneal volume flow

$$\left( \frac{dV}{dt} \text{ or } J_V \right),$$

generated V(t) curves which were in good agreement with predictions based on (approximate) analytical integrations of

$$\left( \frac{dV}{dt} \right)$$

[8]. Thus, the height of the V(t) curves,  $a_1$ , proved to be dependent on the ratio of  $L_pS$  to  $PS_g$  as well as on the glucose concentration and of the volume of the infused dialysis solution. Hence, the height of the curves is largely independent of peritoneal surface area. Furthermore, the peak time of the V(t) curves, was found to be inversely proportional to the  $PS_g$  but directly proportional to intraperitoneal fluid volume. These predictions follow directly from equations 3 and 4.

There are several interesting implications of equations 3 and 4. For example, in children, the V(t) curves for any dialysis fluid glucose concentration would peak earlier than in adults, mainly due to the lower volume of the solution infused. Even though the  $PS_g$  would also be lower in children than in adults, the ratio

$$\frac{\bar{V}}{PS_g} \left[ \frac{\text{volume}}{\text{area}} = \frac{(\text{length scale})^3}{(\text{length scale})^2} \right]$$

would actually be lower too. Hence, the  $t_{peak}$  must be reduced in children (eq. 4), as is also generally observed clinically [35]. An increased L may, however, also contribute to the reduced  $t_{peak}$  seen in children [35].

During peritonitis IPV versus time curves often show changes which are compatible with increases in both small solute PS (and  $PS_g$ ) and in  $L_pS$ . Inasmuch as  $PS_g$  and  $L_pS$  are increased to the same extent, these alterations comply with an increased surface area (S), probably generated by inflammatory recruitment of microvessels (Fig. 5). During peritonitis PS may, however, in some cases increase more than  $L_pS$ , and in this case the curve height is markedly reduced (compare with Fig. 7). The increase of small solute PS (and  $PS_g$ ) occurring in some patients on long-term CAPD treatment are usually also not

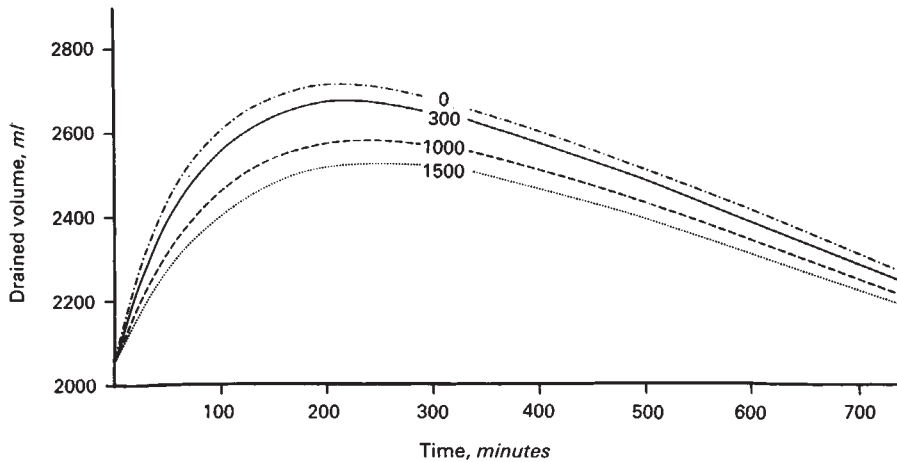


Fig. 9. Simulated  $V(t)$  curves for variations in i.p. residual volume from 0 to 1,500 ml when 2,050 ml of 3.86% Dianeal® is instilled intraperitoneally. Increasing the residual volume will lower the maximum curve height (a) and increase the  $t_{\text{peak}}$ .

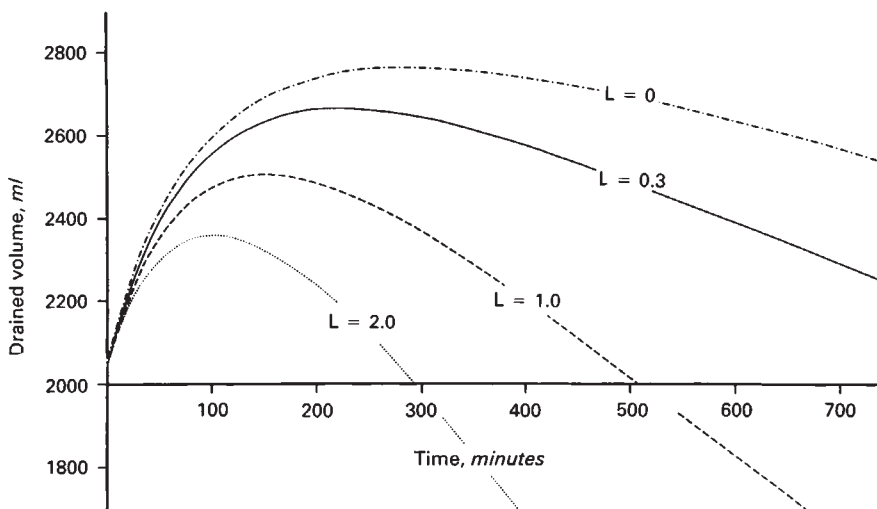


Fig. 10. Impact of lymph flow ( $L$ ) on simulated  $V(t)$  curves using 3.86% glucose in the dialysate infused.  $L$  is varied between zero and 2.0 ml/min. "Control curve" (for  $L = 0.3$  ml/min) is depicted by the solid line.

coupled to increases in  $L_pS$  of the same magnitude, often leading to a marked loss of UF-capacity.

The present model is a "lumped parameter" model treating the blood-peritoneal barrier as a simple membrane analogous to continuous capillary walls. This membrane is assumed to contain two major fluid conductive pathways coupled in parallel, small (paracellular) pores and ultra-small (cell membrane) pores, and a third parallel pathway, large pores, permitting macromolecules to be filtered to the interstitium. The large pore pathway is, however, of negligible importance for fluid transport driven by crystalloid osmosis. More sophisticated models also take into account transport resistances coupled in series. Thus, considering the major peritoneal barrier to be the capillary walls, they also include the interstitium and the mesothelium [25, 26]. Such "distributed model" approaches would be more accurate than the present "single membrane" model. On the other hand they are of much greater complexity [25, 26]. Thus, the present model is easily run on a simple pocket PC.

Distributed models predict the presence of solute concentration gradients in the interstitium throughout the cycle. Hence, according to such models the crystalloid osmotic gradients

acting across the capillary membrane proper will be considerably lower than modelled here. Otherwise the general predictions regarding the  $V(t)$  curves from the present model and from distributed models are similar. However, both distributed models and the present simple parallel pathway model suffer from the problem that they do not accurately predict the concentration of glucose in the dialysate over time, especially after approximately two hours of the cycle (compare with Fig. 3). The rate of dissipation of the apparent "driving" osmotic gradient across the peritoneal barrier in our model and in the distributed model of Seames et al [26] is thus considerably faster than the dissipation rate of the measured i.p. glucose concentration alone. This can only be partly explained by dilution effects following the often massive *transcellular* water movement (UF) occurring during the early phase of the cycle. Such a dilution of the dialysate gradually creates a large sodium chloride (and sodium lactate/bicarbonate) osmotic gradient (Fig. 2) across the peritoneum during the first 50 to 100 minutes of the dwell time. For 3.86% glucose in the dialysis solution, the latter gradient will after 90 minutes become approximately:  $2 \cdot (140 - 118.5) \cdot 19.3 \cdot 0.03 \text{ mm Hg} \approx 25 \text{ mm Hg} (= 2\Delta C_{\text{Na}}$



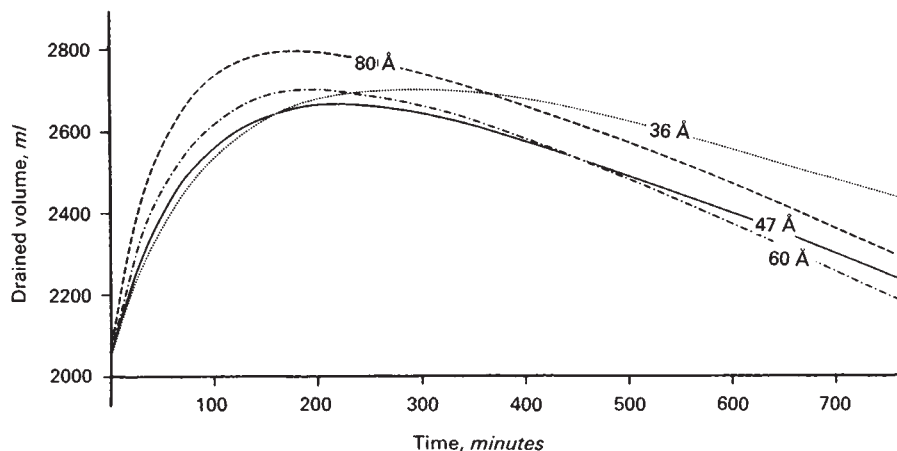


Fig. 11. Theoretical result of varying the small pore radius ( $r_s$ ) on simulated  $V(t)$  curves for 3.86% glucose in the dialysis fluid. Control curve [ $r_s = 47$  (Å)] is denoted by a solid line.

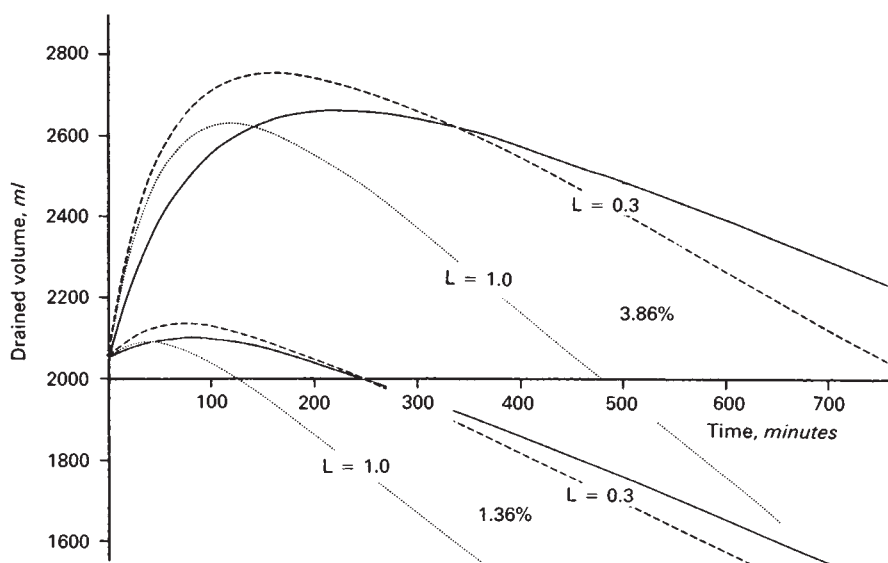


Fig. 12. Effects of "peritonitis" on simulated  $V(t)$  curves for 3.86% glucose (upper three curves) and 1.36% glucose (lower three curves), respectively, in the dialysis fluid. The surface area term ( $S$ ) is increased by 70% and microvascular "permeability" is enhanced by increasing the relative number of large pores one order of magnitude from control. Control curves are represented by solid lines. Lymph flow is either unchanged at 0.3 ml/min (hatched lines) or increased to 1 ml/min (dotted lines).

$RT \cdot \sigma_{\text{NaCl}}$ ), (compare with eq. 6 and 8) in the present simulations. This gradient initially opposes the glucose osmotic gradient, and though it cannot fully explain the rapid dissipation of the driving osmotic gradient over cycle time, it contributes to this phenomenon.

In order to fit our model to previous experimental  $V(t)$  curves during control, which reflect the mentioned rapid dissipation of the driving peritoneal osmotic gradient [8], PS for glucose in this study had to be set approximately 50% higher than predicted from our assumed value of  $A_o/\Delta x$ . A distributed model of peritoneal transport can account for this internal inconsistency between model parameters only if there are marked changes of the interstitial solute concentration profiles with dwell time. Interstitial gradients thus have to become progressively steeper over the course of the cycle, that is, solute transport resistances in the interstitium have to increase with cycle time. One way to conceptualize such alterations is to think of interstitial "unstirred fluid layers" that gradually build up over cycle time due to the decreasing impact over the dwell of transmembrane convection. This may at first seem speculative, but from previously published PET data [1] it seems evident that PS

values for small solutes are 40 to 50% higher during the first 60 minutes of the dwell than subsequently [23]. This would support the notion that "unstirred layers" may actually contribute to peritoneal transport characteristics [2, 4] by gradually building up and enhancing the rate of dissipation of the effective crystalloid osmotic gradient over the course of the cycle. In the present model we have compensated for effects of this kind by increasing the value of  $PS_g$  above that predicted from the assumed value of  $A_o/\Delta x$ .

In the present simulations the peritoneum is considered to be very selective with regard to both solute transport and osmosis (UF). Hence, whereas the ratio of the free diffusion coefficient of glucose ( $9.0 \cdot 10^{-6}$  cm<sup>2</sup>/sec) to that of albumin ( $9.3 \cdot 10^{-7}$  cm<sup>2</sup>/sec) is approximately 10, the ratio of calculated "unidirectional clearances" ( $\approx PS$  values) of these solutes is over 100 (compare with Table 2) for the parameters selected and in agreement with measured clearance data [1, 5-7, 12, 18, 36]. Furthermore,  $\sigma$  for glucose is here 0.043 and that of albumin 0.9, although, due to the heteroporous nature of the peritoneal barrier, the glucose sieving coefficient is as low as 0.6. By contrast, Bell et al [37] found a very low degree of diffusional

**Table 2.** Calculated PS (MTAC) values (assessed using eq. 11 and 12 in ref. 12) and total  $\sigma$ 's (eq. 13, 14) for some solutes as based on the parameters shown in Table 1

	PS ml/min	$\sigma$
Sodium chloride	18.8	0.0262
Urea	16.2	0.0293
Creatinine	13.5	0.0338
Glucose	10.2	0.0430
Albumin	0.086 <sup>a</sup> (0.004)	0.895

$A_0/\Delta X$  is set to 27,000 cm. Note that  $PS_g$  (PS for glucose) calculated in this way is 34% lower than the value (15.5 ml/min) fitting to our previously published  $V(t)$  curves [8]. Solute radius of creatinine was set to 3.0 Å.

<sup>a</sup> Note that the calculated albumin "PS" here represents the "unidirectional clearance" of albumin (comprising both albumin diffusion through small pores and albumin convection through small and large pores) for a net transperitoneal volume flow of 1.0 ml/min (calculated according to the parameters in Table 1). For the three-pore model, a unidirectional clearance of albumin of 0.12 [12] is obtained when  $r_s$  is set at 52 Å. The pure diffusional albumin transport coefficient given in parenthesis is very low.

restriction in the rabbit peritoneum of the passage of different size dextrans, at variance with rabbit dextran clearance data published by others [38–40]. Yet rabbit peritoneal permselectivity with respect to osmosis (UF) was found to be unproportionally high. The sieving coefficients of dextrans across the rabbit peritoneal membrane in their study conformed to a two-pore membrane model comprising a few 300 Å "large pores", accounting for 0.3% of the total pore area, and as much as 43% of the  $L_p S$ , together with a large number of very small pores, 20 Å in radius.

We cannot find that this apparent inconsistency between osmotic and permeation barrier properties of the rabbit peritoneal membrane, exposed to extensive surgery [37], characterizes the normal human blood-peritoneal exchange. It may be explained by methodological differences, species differences and the use of dextrans as molecular probes for membrane selectivity in the rabbit model. Dextrans are long-chained flexible molecules that can "reptate" across pores which are smaller than the Stokes radius of the molecule itself [41].

In conclusion, the present simulations are based on a parallel pathway membrane model derived from capillary physiology, and it comprises a large number of paracellular small pores (radius  $\approx$  45 to 50 Å), accounting for 90 to 95% of the UF-coefficient, and a small number of large pores (radius  $\approx$  250 Å), accounting for  $\approx$ 5% of  $L_p S$ , and, in addition, a "transcellular" fluid conductive pathway, accounting for 1 to 2% of  $L_p S$ . Although it is a simple "lumped parameter" model, easily handled on a pocket PC, it seems to be a useful tool for describing transperitoneal volume shifts during normal and perturbed conditions in CAPD. The presence of transcellular pores offers an explanation of the fact that small solute sieving coefficients in the peritoneal membrane during large glucose induced osmotic UF-flows are approximately 0.5 to 0.7 [42], and not near unity, as predicted by a strict two-pore model [12]. Furthermore, in the present simulations, the peritoneal lymph flow ( $L$ ) was less than 0.5 ml/min, which is consistent with a description of the peritoneal fluid exchange during CAPD in line with current hydrodynamic theories [8].

## Acknowledgments

This study was supported by grants Nos. 8285 and 8796 from the Swedish Medical Research Council.

Reprint requests to Gunnar Stelin, M.D., Department of Nephrology, Sahlgrenska Hospital, S-413 45 Göteborg, Sweden.

## References

1. TWARDOWSKI ZJ, NOLPH KD, KHANNA R, ET AL: Peritoneal equilibration test. *Perit Dialysis Bull* 7:138–147, 1987
2. SMEBY LC, WIDERØE TE, JØRSTAD S: Individual differences in water transport during continuous peritoneal dialysis. *ASAIO J* 4:17–27, 1981
3. WIDERØE TE, SMEBY LC, MJÅLAND S, DAHL K, BERG KJ, AAS TW: Long-term changes in transperitoneal water transport during continuous ambulatory peritoneal dialysis. *Nephron* 38:238–247, 1984
4. WIDERØE TE, SMEBY LC, DAHL K, JØRSTAD S: Definitions of differences and changes in peritoneal membrane transport properties. *Kidney Int* 33(Suppl 24):S107–S113, 1988
5. VERGER C: Relationship between peritoneal membrane structure and its permeability: Clinical implications, in *Advances in Peritoneal Dialysis 1985*, edited by KHANNA R, NOLPH KD, PROWANT B, TWARDOWSKI ZJ, OREOPOULOS DG, Toronto, Toronto University Press, 1985, pp. 87–95
6. KREDIET RT, BOESHOTEN EW, ZUYDERHOUDT FMJ, ARISZ L: Peritoneal transport characteristics of water, low-molecular weight solutes and proteins during long-term continuous ambulatory peritoneal dialysis patients. *Perit Dial Bull* 6:61–65, 1986
7. HEIMBÜRGER O, WANIEWSKI J, WERYNSKI A, TRANÆUS A, LINDHOLM B: Peritoneal transport in CAPD patients with permanent loss of ultrafiltration capacity. *Kidney Int* 38:495–506, 1990
8. STELIN G, RIPPE B: A phenomenological interpretation of the variation in dialysate volume with dwell time in CAPD. *Kidney Int* 38:465–472, 1990
9. HALLETT MD, KUSH RD, LYSAGHT MJ, FARRELL PC: The stability and kinetics of peritoneal mass transfer, in *Peritoneal Dialysis*, edited by NOLPH KD, Dordrecht, Kluwer Academic Publishers, 1989, p. 380
10. JAFFRIN MY, ODELL RA, FARRELL PC: A model of ultrafiltration and glucose mass transfer kinetics in peritoneal dialysis. *Artif Organs* 11(3):198–207, 1987
11. NAKANISHI T, TANAKA Y, FUJII M, FUKUHARA Y, ORITA Y: Nonequilibrium thermodynamics of glucose transport in continuous ambulatory peritoneal dialysis, in *Machine Free Dialysis for Patient Convenience: The Fourth ISAO Official Satellite Symposium on CAPD*, edited by MAEKAWA M, NOLPH KD, KISHIMOTO T, MONCRIEF JW, Cleveland, ISAO Press, 1984, pp. 39–44
12. RIPPE B, STELIN G: Simulations of peritoneal solute transport during continuous ambulatory peritoneal dialysis (CAPD). Application of two-pore formalism. *Kidney Int* 35:1234–1244, 1989
13. RIPPE B, HARALDSSON B: Fluid and protein fluxes across small and large pores in the microvasculature. Application of two-pore equations. *Acta Physiol Scand* 131:411–428, 1987
14. TAYLOR AE, GRANGER DN: Exchange of macromolecules across the microcirculation, in *Handbook of Physiology, The Cardiovascular System IV*, edited by RENKIN EM, MICHEL CC, American Physiological Society, 1984, p. 467
15. CRONE C, LEVITT DG: Capillary permeability to small solutes, in *Handbook of Physiology*, edited by RENKIN EM, MICHEL CC, American Physiological Society, 1984, p. 411
16. RIPPE B, PERRY MA, GRANGER DN: Permselectivity of the peritoneal membrane. *Microvasc Res* 29:89–102, 1985
17. KEDEM O, KATCHALSKY A: Thermodynamic analysis of the permeability of biological membranes to nonelectrolytes. *Biochim Biophys Acta* 27:229–246, 1958
18. PYLE WK, MONCRIEF JW, POPOVICH RP: Peritoneal transport evaluation in CAPD, in *CAPD Update*, edited by MONCRIEF JW, POPOVICH RP, New York, Masson Publishing, 1980, p. 35
19. RIPPE B, STELIN G, AHLMÉN J: Lymph flow from the peritoneal cavity in CAPD patients, in *Frontiers in Peritoneal Dialysis*, edited

- by MAHER JF, WINCHESTER JF, New York, Field, Rich and Assoc Inc, 1986, p. 24
20. LINDHOLM B, HEIMBÜRGER O, WANIEWSKI J, WERYNSKI A, BERGSTRÖM J: Peritoneal ultrafiltration and fluid reabsorption during peritoneal dialysis. *Nephrol Dial Transplant* 4:805-813, 1989
  21. TWARDOWSKI ZJ, PROWANT BF, NOLPH KD, MARTINEZ AJ, LAMPTON LM: High volume, low frequency continuous ambulatory peritoneal dialysis. *Kidney Int* 23:64-70, 1983
  22. PATLAK CS, GOLDSTEIN DA, HOFFMAN JF: The flow of solute and solvent across a two-membrane system. *J Theor Biol* 5:426-442, 1963
  23. RIPPE B, STELIN G, HARALDSSON B: Understanding the kinetics of peritoneal transport, in *Proceedings of the XIth International Congress of Nephrology*, Tokyo 1990
  24. DRAKE R, DAVIS E: A corrected equation for the calculation of reflection coefficients. *Microvasc Res* 15:259, 1978
  25. FLESSNER MF, DEDRICK RL, SCHULTZ JS: A distributed model of peritoneal-plasma transport: Theoretical considerations. *Am J Physiol* 246:R597-R607, 1984
  26. SEAMES EL, MONCRIEF JW, POPOVICH RP: A distributed model of fluid and mass transfer in peritoneal dialysis. *Am J Physiol* 258:R958-R972, 1990
  27. FLESSNER MF, PARKER RJ, SIEBER SM: Peritoneal lymphatic uptake of fibrinogen and erythrocytes in the rat. *Am J Physiol* 244:H89-H96, 1983
  28. MACTIER RA, KHANNA R, TWARDOWSKI ZJ, MOORE H, NOLPH KD: Contribution of lymphatic absorption to loss of ultrafiltration and solute clearances in continuous ambulatory peritoneal dialysis. *J Clin Invest* 80:1311-1316, 1987
  29. NOLPH KD, MACTIER RA, KHANNA R, TWARDOWSKI ZJ, MOORE H, MCGARY T: The kinetics of ultrafiltration during peritoneal dialysis: The role of lymphatics. *Kidney Int* 32:219, 1987
  30. SVENSIÖ E, ROEMPKE K: Microvascular aspects of oedema formation and its inhibition by  $\beta_2$ -receptor stimulants and some other anti-inflammatory drugs, in *Progress in Microcirculation Research II*, edited by COURTICE FC, GARLICK DG, PERRY MA, Sydney, Committee in Postgraduate Medical Education, The University of NSW, 1984, p. 449
  31. FOX J, GALEY F, WAYLAND H: Action of histamine on the mesenteric microvasculature. *Microvasc Res* 19:108-126, 1980
  32. HARALDSSON B, ZACKRISSON U, RIPPE B: Calcium dependence of histamine-induced increases in capillary permeability isolated in perfused rat hindquarters. *Acta Physiol Scand* 128:247-258, 1986
  33. KREDIET RT, ZUYDERHOUDT MJ, BOESHOTEN EW, ARISZ L: Alterations in the peritoneal transport of water and solutes during peritonitis in continuous ambulatory dialysis patients. *Eur J Clin Invest* 17:43-52, 1987
  34. VERGER C, LUGER A, MOORE HL, NOLPH KD: Acute changes in peritoneal transport properties with infectious peritonitis and mechanical injury. *Kidney Int* 23:823-831, 1983
  35. MACTIER RA, KHANNA R, MOORE H, RUSS J, NOLPH KD, GROS-HONG T: Kinetics of peritoneal dialysis in children: Role of lymphatics. *Kidney Int* 34:82-88, 1988
  36. RIPPE B, STELIN G, AHLMÉN J: Basal permeability of the peritoneal membrane during continuous ambulatory peritoneal dialysis (CAPD), in *Advances in Peritoneal Dialysis, Proceedings of the 2nd International Symposium on Peritoneal Dialysis*, edited by GAHL GM, KESSEL M, NOLPH KD, Amsterdam, Excerpta Medica, 1981, p. 5
  37. BELL JL, LEYPOLDT JK, FRIGON RP, HENDERSON LW: Hydraulically-induced convective solute transport across the rabbit peritoneum. *Kidney Int* 38:19-27, 1990
  38. HIRSZEL P, CHAKRABARTI EK, BENNET RR, MAHER JF: Permselectivity of the peritoneum to neutral dextrans. *Trans Am Soc Artif Intern Organs* 30:625-628, 1984
  39. HIRSZEL P, SHEA-DONOHUE T, CHAKRABARTI EK, MONTCALM E, MAHER JF: The role of the capillary wall in restricting diffusion of macromolecules. A study of peritoneal clearance of dextrans. *Nephron* 49:58-61, 1988
  40. ARTHURSON G: Permeability of the peritoneal membrane, in *6th European Conference on Microcirculation, Aalborg, 1970* Basel, Karger, p. 197, 1971
  41. MUNCH WD, ZESTAR LP, ANDERSON JL: Rejection of polyelectrolytes from microporous membranes. *J Membr Sci* 5:77-102, 1979
  42. HENDERSON LW, LEYPOLDT JK: Ultrafiltration with peritoneal dialysis, in *Peritoneal Dialysis* (3rd ed), edited by NOLPH KD, Dordrecht, Kluwer Academic Publishers, 1989, p. 117